Towards Model-Based Geometry Reconstruction of Quantum Dots from TEM

Thomas Koprucki*, Anieza Maltsi*, Tore Niermann:†, Timo Streckenbach*, Karsten Tabelow*, Jörg Polzehl*
* Weierstrass Institute (WIAS), Mohrenstr. 39, 10117 Berlin, Germany
† Institut für Optik und Atomare Physik, Technische Universität Berlin, Strae des 17. Juni 135, 10623 Berlin

Email: thomas.koprucki@wias-berlin.de

***Abstract*—We present a novel concept for 3D model-based geometry reconstruction (MBGR) of semiconductor quantum dots (QDs) form imaging of bulk-like samples (thickness 100-300 nm) by transmission electron microscopy (TEM). The approach includes an appropriate model for the QD configuration in real space, a database of simulated TEM images and a statistical procedure for the estimation of QD properties and classification of QD types based on machine learning techniques. For the numerical simulation of TEM images we use an elasticity solver to obtain the strain profile, which enters a solver for the Darwin-Howie-Whelan equations, describing propagation of the electron wave through the sample.**

I. Introduction

The growth of semiconductor quantum dots (QDs) with desired electronic properties would highly benefit from the assessment of QD geometry, distribution, and strain profile in a feedback loop between epitaxial growth and analysis of their properties. To assist the optimization of QDs imaging by transmission electron microscopy (TEM) can be used. However, a direct 3D geometry reconstruction from TEM of bulk-like samples, see Fig. 1, by solving the tomography problem is not feasible due to its limited resolution (0.5-1 nm), the highly nonlinear behaviour of the dynamic electron scattering and strong stochastic influences due to uncertainties in the experiment, e.g. excitation conditions.

Here, we present a novel concept for 3D model-based geometry reconstruction (MBGR) of QDs from TEM images. This will include (a) an appropriate model for the QD configuration in real space including a categorization of QD shapes (e.g., pyramidal or lense-shaped) and continuous parameters (e.g., size, height), (b) a database of simulated TEM images covering a large number of possible QD configurations and image acquisition parameters (e.g. bright field/dark field, sample tilt), as well as (c) a statistical procedure for the estimation of QD properties and classification of QD types based on acquired TEM image data. In order to develop the mathematical methods for MBGR we will focus on InAs QDs in a GaAs matrix and consider TEM imaging also sensitive to elastic strain.

II. Simulation of TEM images

The propagation of the electron wave through the specimen is governed by the relativistic Schrödinger equation [1]. The dynamic electron scattering in crystalline solids, e.g., semiconductor nanostructures, is influenced by spatial variations in the chemical composition and by local deformations of the lattice due to elastic strain. By variation of the excitation conditions the sensitivity of the imaging can be tuned, e.g. to different components of the strain as shown in Fig. 1.

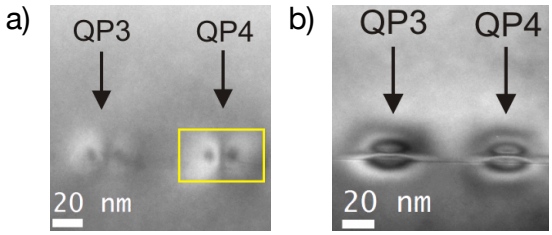

Fig. 1. TEM images of InAs QDs: (a) dark field of (040) reflection, sensitive to [010]-component of strain (b) dark field of (004) reflection, sensitive to [001]-component of strain, see [2], both showing a coffee-bean-like contrast.

The spatial domain of sample is denoted by $\Omega \subset \mathbb{R}^3$, and the part containing the QD by $\Omega_{\mathrm{QD}} \subset \Omega$. We model the QD geometry by a spatial profile of a indium mole fraction $c(\mathbf{r})$ of an virtual $\mathrm{In_xGa_{1-x}As}$ alloy, and set $c(\mathbf{r}) = 1$ for $\mathbf{r} \in \Omega_{\mathrm{QD}}$ and $c(\mathbf{r}) = 0$ elsewhere.

A. Elastic relaxiation of misfit induced strain

The InAs QDs under consideration and the surrounding GaAs matrix have different lattice constants, $a^{\mathrm{InAs}} > a^{\mathrm{GaAs}}$, and this induces mechanical stresses in the nanostructure. To model the elastic relaxation of the misfit-induced strain we employ continuum mechanics. The strain tensor is defined as $\boldsymbol{\varepsilon}(\mathbf{u}) = \frac{1}{2}\left(\nabla\mathbf{u} + (\nabla\mathbf{u})^T\right)$ by the displacement $\mathbf{u}$ and the stress is connected to the strain by Hook's law: $\boldsymbol{\sigma} = \mathbf{C} : \boldsymbol{\epsilon}$, where $\mathbf{C}$ is the elastic stiffness tensor. To model the elastic relaxation of the misfit-induced strain ε_m we are following the concept of Eshelby's inclusion [3]: The eigen strain is given by $\boldsymbol{\varepsilon}^*(\mathbf{r}) = \varepsilon_m \delta_{ij}$ for $\mathbf{r} \in \Omega_{QD}$ and $\boldsymbol{\varepsilon}^* = 0$ elsewhere, and the eigen stress as $\boldsymbol{\sigma}^* = \mathbf{C} : \boldsymbol{\varepsilon}^*$. The displacement field $\mathbf{u}$ of the equilibrium configuration is obtained by solving:

$$\nabla \cdot (\boldsymbol{\sigma} - \boldsymbol{\sigma}^*) = 0 \text{ in } \Omega \tag{1}$$

with $(\boldsymbol{\sigma} - \boldsymbol{\sigma}^*) \cdot \mathbf{n} = 0$ on the part of the boundary of Ω describing free surfaces ($\mathbf{n}$ denotes the normal to the boundary) and homogenous Dirichlet boundary conditions on the remaining part. Results obtained with a FEM-based elasticity solver for a spherical and a pyramidal QD are shown in Fig. 2.

978-1-5386-5599-3/18/$31.00 ©2018 IEEE

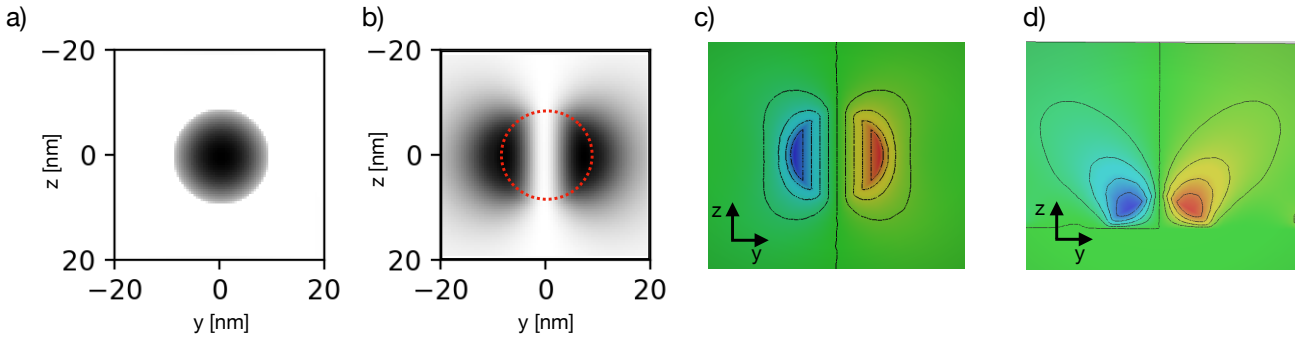

Fig. 2. Simulated TEM images for InAs sphere with radius 10 nm embedded in a GaAs matrix: (a) bright field for chemical contrast only (b) bright field also including influence of strain. The image contrast in (a) in strongly increased for better visualisation. Due to the excitation under (040) strong beam conditions, the image contrast is sensitive to the [010]-component of the displacement field corresponding to u_y obtained by FEM simulations. The observed coffee-bean contrast looks qualitatively similar to the experimental results shown in Fig.1a. u_y component of the displacement field along a yz-cross-section through the center of the QDs from FEM simulation of the elastic relaxation: (c) InAs sphere in GaAs matrix (d) pyramidal InAs QD in GaAs matrix. The TEM images (a) and (b) have been simulated with pyTEM [7], assuming analytical approximation of the displacement field. The crossections of the u_y component of the displacement field along a yz-plane through the center of the QDs have been obtained with the FEM-based elasticity solver of WIAS-PDELIB [6].

B. Dynamical electron scattering

We use an multi-beam ansatz for the wave function

$$\Psi(\mathbf{r}) = \sum_{\mathbf{g}} \psi_{\mathbf{g}}(z;x,y) e^{2\pi i(\mathbf{k}_0+\mathbf{g})\cdot\mathbf{r}}, \tag{2}$$

where $\mathbf{k_0}$ describes the incoming electron beam and $\mathbf{g}$ is a vector in the reciprocial lattice. Due to the column approximation the amplitudes $\psi_{\mathbf{g}}$ depend only parametrically on the (x,y)-coordinates, which define a 2D pixel array constituting the TEM image. We consider only amplitudes $\psi_{\mathbf{g}}$ with an small excitation error $s_{\mathbf{g}} = -\frac{\mathbf{g}\cdot(2\mathbf{k}_0+\mathbf{g})}{2n\cdot(\mathbf{k}_0+\mathbf{g})}$. In combination with the column approximation the multi-beam ansatz leads to the Darwin-Howie-Whelan equations [1]

$$\frac{d\psi_{\mathbf{g}}}{dz} = i\pi \sum_{\mathbf{g}'} \left[2s_{\mathbf{g}}\delta(\mathbf{g}-\mathbf{g}') + U_{\mathbf{g}-\mathbf{g}'}\right]\psi_{\mathbf{g}'} \tag{3}$$

where the Fourier coefficients $U_{\mathbf{g}}$ of reduced electrostatic potential $U(\mathbf{r})$ of the crystal describe the coupling between the beams. For displacement fields $\mathbf{u}(\mathbf{r})$ which are nearly constant on length scales $1/g$ The influence of lattice deformations on the scattering can approximated by the modification

$$U_{\mathbf{g}} \to U'_{\mathbf{g}}(\mathbf{r}) = U_{\mathbf{g}} \exp(2i\pi\mathbf{u}(\mathbf{r})\cdot\mathbf{g}), \tag{4}$$

where $\mathbf{u}(\mathbf{r})$ is the displacement field. Only the projection of the displacement field on the individual reciprocial lattice vector g enters the coupling term. A simulated TEM image is constituted by propagating the beams through the sample for every pixel (x_i, y_j), $i,j = 1,\ldots,N$, by numerically solving Eq. (3) using the displacements fields computed by the elasticity solver. Fig. 2b shows a simulated TEM image for a spherical QD, revealing a coffee-bean like contrast which looks similar to the experimental results shown in Fig. 1a. For comparison Fig 2a shows an artificial TEM image using the effect of the chemical contrast only, neglecting strain effects. Even the qualitative behaviour differs strongly from Fig. 2b and from the experimental observations emphasizing the importance of the coupled simulation for obtaining realistic results.

III. Model-based geometry reconstruction

The ultimate goal of our approach is the reconstruction of the geometry of QDs from measured TEM images. We will start analysing the properties of simulated TEM images that are generated by the methods described above. The problem contains two parts: a) determination of the class or type of QD geometries b) the estimation of continuous parameters like size, height or depth of the QD. Provided that the database of simulated TEM images is large enough we will train a convolutional neural network to solve the classification problem. Accompanying we will study the structure of the image space by means of elastic shape analysis [4], [5] in order to establish inference methods for geometric properties of the quantum dots. Both topics are under investigation and we will present our current state of understanding at the conference along with results on the database of simulated TEM images.

Acknowledgment

This work received funding from the Einstein Center for Mathematics Berlin under project MATHEON-OT7 (A.M.) and from DFG within CRC 787 "Semiconductor Nanophotonics" under projects A4 (T.N.) and B4 (T.K.).

References

[1] M. De Graef,"Introduction to conventional transmission electron microscopy," Cambridge University Press, 2003.
[2] M. Hartwig, "TEM-Untersuchungen der Spannungsfelder von In(Ga)As-Quantenpunkten," Bachelor thesis, TU Berlin, December 2011.
[3] J.D.Eshelby, "The Determination of the Elastic Field of an Ellipsoidal Inclusion, and Related Problems," *Proc. R. Soc. London A: Math. Phys. Eng. Sci.* vol. 241, p. 376 – 396, 1957.
[4] S. Kurtek and H. Drira, "A comprehensive statistical framework for elastic shape analysis of 3d faces," *Computers & Graphics*, vol. 51, pp. 52 – 59, 2015.
[5] S. Kurtek et al, "Elastic Shape Analysis of Surfaces and Images,", pp. 257–277, In P.K. Turaga and A. Srivastava, editors, *Riemannian Computing in Computer Vision*, Springer International Publishing, 2016.
[6] J. Fuhrmann, T. Streckenbach et al, *http://pdelib.org*. [Software]
[7] T. Niermann, *pyTEM*. [Software]